# Characterization of preconcentrated domestic wastewater toward efficient bioenergy recovery: Applying size fractionation, chemical composition and biomethane potential assay

Yuan Yang[a], Yisong Hu[a,c,e*], Ao Duan[a], Xiaochang C. Wang[a,b,c], Huu Hao Ngo[c,d], Yu-You Li[e]

[a] Key Lab of Northwest Water Resource, Environment and Ecology, MOE, Xi'an University of Architecture and Technology, Xi'an 710055, P.R. China

[b] Key Lab of Environmental Engineering, Shaanxi Province, Xi'an 710055, P.R. China

[c] International Science & Technology Cooperation Center for Urban Alternative Water Resources Development, Xi'an 710055, P.R. China

[d] Centre for Technology in Water and Wastewater, School of Civil and Environmental Engineering, University of Technology Sydney, Sydney, NSW 2007, Australia

[e] Department of Civil and Environmental Engineering, Graduate School of Environmental Studies, Tohoku University, 6-6-06 Aza-Aoba, Aramaki, Aoba-ku, Sendai, Miyagi 980-8579, Japan

*Corresponding author: Y. Hu (Tel.: +862982205652; E-mail: huyisong@xauat.edu.cn)

**Abstract** Domestic wastewater (DWW) can be preconcentrated to facilitate energy recovery via anaerobic digestion (AD), following the concept of "carbon capture–anaerobic conversion–bioenergy utilization." Herein, real DWW and preconcentrated domestic wastewater (PDWW) were both subject to particle size fractionation (0.45–2000 μm). DWW is a type of low-strength

wastewater (average COD of 440.26 mg/L), wherein 60% of the COD is attributed to the substances with particle size > 0.45 μm. Proteins, polysaccharides, and lipids are the major DWW components. PDWW with a high COD concentration of 2125.89 ± 273.71 mg/L was obtained by the dynamic membrane filtration (DMF) process. PDWW shows larger proportions of settleable and suspended fractions, and accounted for 63.4% and 33.8% of the particle size distribution, and 52.4% and 32.2% of the COD, respectively. The acceptable biomethane potential of 262.52 ± 11.86 mL $CH_4$/g COD of PDWW indicates bioenergy recovery is feasible based on DWW preconcentration and AD.

**Keywords:** domestic wastewater preconcentration; resource recovery; bioenergy production; biomethane production potential; carbon capture

## 1. Introduction

In recent years, due to the rapid growth of population and expansion of urbanization, the generation of domestic wastewater (DWW) together with the fossil energy consumption in wastewater treatment have increased. In wastewater treatment with the conventional activated sludge (CAS) process, up to 60% of the operating cost is due to the energy consumption (Yang et al., 2020a). In many developed countries, 1–4% of the total electricity budget is attributable to municipal wastewater treatment (Sarpong et al., 2019). Actually, DWW is now considered as a resource for water, energy, and nitrogen and phosphorus nutrients, rather than as a waste (McCarty et al., 2011). Recently, recovering resources and energy contained in wastewater has attracted much academic attention. Topics include phosphorus and nitrogen recovery, wastewater reclamation,

anaerobic digestion (AD) of excess sludge, as well as the microbial fuel cell (MFC) technology for electricity production (Liu et al., 2020; Joel and Okabe, 2020).

Additionally, energy contained in wastewater can be recovered directly as methane-rich biogas through anaerobic digestion, which has been proven to be a mature and practical method for achieving net energy production and meeting stringent wastewater discharge standards (McCarty et al., 2011; Lei et al., 2018; Hu et al., 2018). However, DWW is a low-strength wastewater, which makes direct anaerobic treatment of such wastewater less economically feasible at temperate climates (Jin et al., 2015). If the diluted organic matters in DWW can be captured and enriched in the preconcentrated domestic wastewater (PDWW) via reasonable processes, the cost-effective production of biogas from DWW can be expected to be achieved. Nowadays, aiming to achieve organics enrichment for energy recovery, wastewater preconcentration techniques, including a variety of biological and physicochemical processes, have received broad interest. Among these, bioflocculation and flocculation methods, such as high-rate activated sludge (HRAS) and chemically enhanced primary treatment (CEPT), have been investigated widely (Meerburg et al., 2016). Currently, the membrane filtration systems have been considered as a compact and feasible process for low-strength wastewater preconcentration, including microfiltration (MF), ultrafiltration (UF), forward osmosis (FO) and dynamic membrane (DM) (Liu et al., 2020; Gao et al., 2018; Xiong et al., 2019). Such means show a significant organics retention efficiency with much lower requirements of aeration and chemicals, thus the high-quality concentrates

with high COD content can be obtained. Researchers also combined HARS and CEPT with various membrane systems to develop more efficient wastewater preconcentration processes (Jin et al., 2015; Faust et al., 2014; Lateef et al., 2013).

However, the characteristics of real wastewater always vary with its origins, which is different from the case of synthetic wastewater containing mainly known biodegradable substances. For example, the total COD of municipal wastewater was 480 ± 110 mg/L, with particulate, colloidal and soluble COD accounting for 60%, 16.7% and 22%, respectively (Jimenez et al., 2015). While in another study, the suspended, colloidal and soluble COD fractions of municipal wastewater was measured as 34%, 25% and 39%, respectively (Hernández Leal et al., 2011). Understanding the physicochemical properties of raw wastewater, especially the chemical composition associated with the particulate size distribution, is a prerequisite for the design of wastewater preconcentration processes toward material and energy recovery. Meanwhile, the properties of wastewater concentrate are different depending on the wastewater source and preconcentration processes among others. Gao et al. obtained the sewage concentrate with high COD concentration of 2714.4–3288.6 mg/L and methane conversion over 70% by FO process, and concluded that the enriched ammonia nitrogen ($NH_3$-N) and salinity caused by salt reverse osmosis might inhibit the biogas production (Gao et al., 2019). Lateef et al. performed the direct MF filtration of municipal wastewater to get the concentrate with COD of 2500–5000 mg/L (Lateef et al., 2013), while the membrane fouling control method (chemically enhanced backwash) made the

process complicated and the continuous aeration applied may induce the mineralization of COD in wastewater. Jin et al. conducted sewage preconcentration by a combined coagulation-MF system, and COD of the concentrate reached 16000 mg/L in 295 h. However anaerobic biodegradability of the concentrate was only 56.5%, which may be affected by polyaluminum chloride (PAC) accumulation in the concentrate to some extent (Jin et al., 2016). Above researches indicate that the characteristics of preconcentrated wastewater are variable and biogas production potential cannot be predicted precisely due to the complex composition of enriched organics. Hence it is necessary to comprehensively characterize the obtained concentrate. The preconcentration mechanism and material/energy recovery efficiency should be revealed, to support better design and optimization of wastewater preconcentration processes. However, as far as we know, only limited studies have addressed aforementioned issues, while no other work has made a detail comparison between raw wastewater and the preconcentrated wastewater based on size fractionation.

In our previous study, it was proved that real DWW could be effectively concentrated by a dynamic membrane filtration (DMF) process (Xiong et al., 2019). Therefore, the objectives of this study are as follows: 1) to sieve DWW and PDWW into several fractions from less than 0.45 μm to 2000 μm, and analyze the detailed components of each; 2) to verify the energy recovery efficiency of the wastewater concentrate by carrying out methane production potential experiments using the PDWW with different particle size ranges as the substrate; and 3) to provide some useful technical

implications for efficient bioenergy recovery from DWW.

## 2. Materials and methods

### *2.1. DWW preconcentration using the DMF process*

The real DWW for preconcentration was obtained from a local wastewater treatment plant (WWTP) in Xi'an, China. The DWW had a total COD of 440.26 ± 36.35 mg/L, a soluble COD (SCOD) of 191.83 ± 34.70 mg/L, a dissolved organic carbon (DOC) of 86.37 ± 16.31 mg/L, a total nitrogen (TN) of 41.50 ± 3.68 mg/L, a $NH_3$-N of 34.56 ± 4.47 mg/L, a total phosphorus (TP) of 4.88 ± 0.52 mg/L, a phosphate phosphorus ($PO_4^{3-}$-P) of 3.25 ± 0.26 mg/L, and a chroma of 187.16 ± 20.41 c.u. The DWW was preconcentrated by applying a DMF reactor based on our previous work (Xiong et al., 2019). In brief, the raw DWW was fed into the reactor with a DM module, with a two-layer stainless-steel mesh with pore size of 25 μm as the supporting material. The effluent was extracted continuously by a peristaltic pump at a stable flux of 50–60 L/$m^2$h with each filtration cycle lasting about 48 h. No periodic relaxation or backwashing was conducted due to the good DMF filtration performance.

### *2.2. Fractionation of DWW and PDWW*

Size fractionation of both raw DWW and PDWW was carried out to explore the distribution of basic parameters such as organic and nutrients concentrations and others over the particle sizes. All samples were fractionated within 1 hour directly on site for further analysis. In the case of delay of sample measurement at the laboratory, the

fractionated samples were kept at 4 °C to prevent changes in wastewater composition. The measurement of all basic parameters, including COD, TN, TP, total suspended solids (TSS), volatile suspended solids (VSS) and biomethane potential (BMP) tests were carried out immediately after the sample well fractionated. The samples were prepared for X-ray photoelectron spectroscopy (XPS) and scanning electron microscopy (SEM)-energy diffusive X-ray (EDX) analysis at the same time.

The detailed fractionation procedure is presented in Fig. 1, 3 L of DWW/PDWW was firstly fractionated over a clean stainless-steel sieve (pore size of 2000 μm) to remove large particles. The remaining filtrate was fractionated by another stainless-steel sieve with smaller pores (105 μm). Subsequently, the filtrate was fractionated step-by-step using filter papers with a decreased pore size from 40 μm to 10 μm, 5 μm, and 0.45 μm. In each procedure, 0.5 L filtrate was collected for further analysis, and the residual was used for the next fractionation step. This size fractionation was completed in a 300 mL ultrafiltration device (MSC300, Mosu, Inc., China), with the stirring rate of 100 rpm and the $N_2$ pressure controlled at 0.01 MPa. In this study, the raw DWW and raw PDWW were considered to be the filtrates with particle size less than 2000 μm (fractionated by steel stainless sieves with a pore size of 2000 μm). The substances in the different fractions with particle sizes of 40–2000 μm, 5–40 μm, 0.45–5 μm and less than 0.45 μm were considered as the settleable, suspended, colloidal, super colloidal, and dissolved substances, respectively (van Nieuwenhuijzen et al., 2004). The comparisons between the DWW and PDWW (Section 3.3), and BMP assay (Section

3.5) were based on such a classification.

**Fig. 1.**

## *2.3. Physical and chemical composition analysis*

### 2.3.1. Conventional parameters analysis

The raw DWW and PDWW concentrates after 2000 μm fractionation were subjected to particle size distribution (PSD) analysis, which was performed by a laser granularity distribution analyzer (LS 230/SVM+, Beckman Coulter Corporation, USA) with a detection range of 0.45–2000 μm. All the filtrates of the different fractionation steps were analyzed for turbidity, chroma, COD, SCOD, TN, TP, TSS, VSS, polysaccharide (PS), protein (PN), and lipid (Lip). Samples following 0.45 μm filter filtration were measured for SCOD, DOC, $NH_3$-N and $PO_4^{3-}$-P. Turbidity was measured using a turbidity meter (2100Q, HACH, USA), and chroma was measured using a chroma meter (SD, 9001, China). The pH values were measured using a potable pH meter (Horiba, Kyoto, Japan). Measurements of COD, SCOD, DOC, TN, TP, $NH_3$-N, $PO_4^{3-}$-P, TS, VS, TSS, VSS, and Lip were conducted according to the standard methods (N.E.P.A. Chinese, 2002). PS and PN were determined using the Anthrone method (Gaudy, 1962) and the Lowry–Folin method (Lowry et al., 1951), respectively, with glucose and bovine serum albumin (BSA) used as standards for the measurements of PS and PN, respectively. Concentrations of PS, PN and Lip were transformed to COD equivalents based on an assumed typical molecular formula such as $C_6H_{12}O_6$, $C_{14}H_{12}O_7N_2$, and $C_8H_6O_2$, which led to the production of 1.06 g of COD, 1.2 g of COD, and 2.03 g of

COD for 1 g of polysaccharide, 1 g of protein, and 1 g of lipid, respectively (Sophonsiri and Morgenroth, 2004).

2.3.2. Morphology and elemental composition of TS in PDWW

Photographs of the stainless-steel sieve and filter papers used in the filtration process were taken by a cinema camera. To observe the morphology and explore the elemental composition of TS in PDWW further, a 200 mL filtrate of each fraction of PDWW was dried in an oven at 105 °C to remove the moisture in the TS for further analysis (Gao et al., 2011). The morphology of the dried TS was observed by SEM analyzer (MLA650F, FEI, USA), and then EDX analysis (Inca 300, United Kingdom) was performed after the SEM images were obtained. The elemental composition of the TS in PDWW was detected by X-ray photoelectron spectroscopy (XPS; Perkin-Elmer PHI 5000C ESCA) using Al K radiation. The binding energy (BE) values were calibrated using C 1s = 284.6 eV as a reference. The XPS data were analyzed using the Auger Scan 320 Demo software.

## *2.4. BMP test*

A slightly modified BMP test was carried out to assess the potential of bioenergy recovery of the different fractions of the PDWW according to previous studies (Xiong et al., 2019). In detail, the BMP assay was performed in 120 mL serum bottles placed in a shaking bath, and the temperature was set at 37 ± 1 °C. The inoculated sludge was collected from a lab-scale anaerobic bioreactor treating real DWW (Yang et al., 2020b), and a three–days starvation treatment was implemented before use. The MLSS of the

inoculated sludge in each bottle was controlled at a concentration of approximately 5 g/L, and with volume of 20 mL. A 60 mL volume of PDWW filtrate of the fractions of <2000 μm, <105 μm, <40 μm, <10μm, <5 μm, and <0.45 μm was added in each bottle. Thus, the total working volume was 80 mL. Air in the headspace of each bottle was purged by nitrogen gas for 2 min. After 1 min of running the test, the pressure caused by thermal expansion in the headspace of the serum bottles was released using a syringe. The cumulative gas production was calculated by measuring the increase of gas volume with a glass syringe along with the cultivation time. The composition of the biogas was measured frequently by a gas chromatograph (GC7900, Tianmei, China) equipped with a thermal conductivity detector (TCD) and a packed column (TDX-01, Shanghai Xingyi Chrome, China) (Xiong et al., 2019). To better explore the BMP of the PDWW fraction with different particle size, the data were exhibited as settleable, suspended, colloidal, and dissolved fractions instead of the different sieving fractions. Duplicate BMP tests were conducted and the average values were reported.

## *2.5. Data analysis*

Correlation analysis was conducted using the Pearson product-moment correlation coefficient ($r_p$, Eq. (1)):

$$r_p = \frac{\Sigma(x - x_{avg})(y - y_{avg})}{\sqrt{\Sigma(x - x_{avg})^2 (y - y_{avg})^2}} \quad (1)$$

where the value of $r_p$ varies between −1 and +1, $r_p = 0$ indicates no correction, whereas $r_p = -1$ or $r_p = +1$ indicates a perfect correlation. If $-0.4 < r_p < +0.4$, the correction is assumed to be weak and is ignored. Positive $r_p$ indicates a direct

proportionality, and negative $r_p$ indicates an inverse proportionality. The $x$ and $y$ are samples of paired data, and the mean values are expressed as $x_{avg}$ and $y_{avg}$ (Zhou et al., 2017). The data were analyzed by using the SPSS version 20.0 software (SPSS Software, Chicago, IL, USA).

The experimental data of the BMP of the PDWW were simulated using the modified Gompertz equation (Eq. (2)):

$$P = P_0 \cdot exp\left\{ -exp\left[\frac{R_{\max} \cdot e}{P_0} \cdot (t_0 - t) + 1\right]\right\} \quad (2)$$

where $P$ means methane production (mL), $P_0$ represents methane production potential (mL), $R_{max}$ indicates the maximum methane production rate (mL/d), $t_0$ is the lag time (days), and $e$ = 2.718281828. Origin 8.5 software (Origin Lab Corporation, USA) was used to fit the methane production curve (Wang et al., 2018). Taking into account the different COD concentration of different group of the PDWW, the unit of $P_0$ and $R_{max}$ were converted into mL $CH_4$/g COD and $CH_4$/g COD/d in discussion (Section 3.5).

## 3. Results and discussion

### *3.1. Basic parameters of raw DWW*

Fig. 2 presents the basic characteristics of the different size fractions from the DWW. The PSD result shows that most of the suspended solids (SS) in the DWW were larger than 10 μm, with a mean diameter as 44.13 μm and a median diameter of 47.36 μm. The chroma of the fraction of DWW with SS particle size less than 5 μm was 26.25 ± 3.51 c.u., and the chroma value of the raw DWW was as high as 187.49 ± 20.41 c.u.,

indicating that the SS with particle size greater than 5 μm in the DWW was the main contributor to chroma; this result corresponded well with the turbidity result. The concentrations of TSS and VSS of the DWW fractions declined with the decrease in the fractionation size. In the raw DWW, the concentrations of TSS and VSS were 170.23 ± 10.11 mg/L and 120.69 ± 12.36 mg/L, respectively, which were comparable to the values obtained in previous studies (Sun et al., 2016; Da Ros et al., 2020). Furthermore, the ratio of VSS/TSS was 0.71 in the DWW, suggesting that the SS were composed mainly of organic matters.

The COD of the raw DWW reached 440.23 ± 36.35 mg/L, and the SCOD concentration was 191.83 ± 34.70 mg/L. The main components of the COD were organic substances such as polysaccharides, proteins, and lipids, which is consistent with the results of other studies (Sophonsiri and Morgenroth, 2004; Huang et al., 2010). The concentration of polysaccharides in the DWW was 18.26 ± 1.11 mg/L, and it was mainly in dissolved form (concentration of 10.11 ± 2.17 mg/L). The concentrations of lipids and proteins in the DWW were relatively high, reaching 69.23 ± 13.98 mg/L and 218.40 ± 11.14 mg/L, respectively. Unidentified COD, defined as the difference between the measured total COD and the sum of the identified COD fractions, was labelled as “others”. “Others” may include humic acid, volatile fatty acids, tannic acid, and even nucleic acid and so forth. Moreover, organic matters such as fiber, starch, and lignin also contributes to COD (Huang et al., 2010; Ravndal et al., 2018). As shown in Fig. 2 (d), SCOD only accounted for 40% of the total COD, and proteins and lipids in

the DWW existed mainly as matters with larger particle sizes (> 10 μm). Meanwhile, the high relationship between COD and TSS ($r_p$ = 0.865) indicates that COD in DWW can be effectively concentrated and enriched if particle fraction can be intercepted.

Fig. 2 (e) shows the concentration of TN and TP of all fractions. In the raw DWW, the concentrations of TN and TP were 41.50 ± 3.68 mg/L and 4.88 ± 0.52 mg/L, respectively, and most of the nitrogen and phosphorus were in the dissolved form (< 0.45 μm). Nitrogen was dominated by $NH_3$-N with a concentration of 34.56 ± 4.47 mg/L, and phosphorus was mainly in the form of $PO_4^{3-}$-P with a concentration of 3.25 ± 0.26 mg/L. The slightly increasing trend of TN and TP concentration confirms the proportion of substances containing phosphorous and nitrogen (e.g., phospholipids and proteinaceous substances) may be larger for lower size fractions in the wastewater (van Nieuwenhuijzen et al., 2004; Ravndal et al., 2018); this can be supported by significant correlations between the concentrations of TN and proteins ($r_p$ = 0.915), and the concentrations of TP and lipids ($r_p$ = 0.829). Moreover, Fig. 2 (f) shows that the corresponding ratios of COD/TN and COD/TP in different fractions increased with increasing sieve size, which is consistent with the results of previous studies (van Nieuwenhuijzen et al., 2004; Da Ros et al., 2020). This phenomenon verifies that more COD is related to larger particles compared to nitrogen and phosphorous.

**Fig. 2.**

## *3.2. Composition of the PDWW*

The basic characteristics of PDWW are presented in Fig. 3. The PSD result shows

that DM filtration can be a feasible method for obtaining PDWW. The diameter of particles in the PDWW was mostly in the range of 67–1000 μm, with a mean particle size of 113.3 μm. The effective accumulation of SS caused a significant increase of chroma to 913.44 ± 67.28 c.u. The chroma of the PDWW with filter size smaller than 105 μm was 494.51 ± 47.25 c.u., indicating that large particles between 105 and 2000 μm mainly induced the chroma in the PDWW, which also corresponded well with the turbidity of the PDWW. The TSS and VSS concentrations increased to 950.63 ± 80.25 mg/L and 694.43 ± 60.69 mg/L, respectively; the TSS of the PDWW fraction with size less than 40 μm was 460.11 ± 97.36 mg/L, indicating that SS with particle size greater than 40 μm was the major proportion. The ratio of VSS/TSS in the PDWW was 0.73, suggesting that the intercepted large-size SS contained abundant organic substances.

The COD of the PDWW was 2125.89 ± 273.71 mg/L, and the concentrations of polysaccharides, proteins, and lipids were 79.03 ± 9.31 mg/L, 844.74 ± 101.88 mg/L, and 77.79 ± 4.32 mg/L, respectively, which existed mainly in particles larger than 10 μm. It is worth noting that particles between 105–2000 μm contains a significant proportion of the COD (concentration of 1021.89 ± 145.22 mg/L), and COD referred to "others" accounting for a large proportion. The high COD composition as "others" with large particle size of PDWW, possibly due to the humic acid, volatile fatty acids, tannic acid, and even nucleic acid, as well as the sources of solid substances in DWW, such as toilet papers and food residues, which can be preconcentrated effectively thus contributing to the COD of the large-sized fraction (Dignac et al., 2000; Huang et al.,

*2010; Eriksson et al., 2002).*

*The DM filtration process retained the large particulates, however, the concentration of SCOD was only 286.80 ± 34.52 mg/L, which verified the poor interception of the dissolved matter by DM filtration. Similar phenomena were observed for TN and TP. In this study, the dissolved nitrogen and phosphorus contents in the PDWW were similar to those of the DWW; however, the concentrations of TN and TP in the PDWW increased to 72.11 ± 4.73 mg/L and 11.86 ± 1.01 mg/L, which were 1.74 and 2.42 times the TN and TP of the DWW, respectively, indicating that the nitrogen and phosphorus associated with particles can be effectively preconcentrated via the DMF process. The sewage concentrate with a COD of 2714.4–3288.6 mg/L, TN of 260.3–293.6 mg/L ($NH_3$-N of 190.3–224.2 mg/L), and TP of 77.3–79.9 mg/L could be obtained with the FO process due to the high retention capacity of the FO membrane (Gao et al., 2018). While in the research of Ortega-Bravo et al., the COD concentration in wastewater concentrate reached 8089 mg/L; however, the concentration factors for $NH_3$-N were negative for wastewater and filtrated wastewater in the FO concentrate. This can be explained by the weak interception of $NH_3$-N in the feed compartment by the membrane or partially due to $NH_3$-N desorption during the concentration process (Ortega-Bravo et al., 2016). The above-mentioned analysis that indicates the interception efficiency of COD, TN, and TP depended on many factors, such as the membrane and sewage properties; thus, the concentration behavior cannot be generalized.* Furthermore, the concentration of nitrogen corresponded well with protein ($r_p$ =

0.945); similarly, the phosphorus concentration corresponded well with the lipids content ($r_p$ = 0.974). Fig. 3 (f) shows that the ratios of COD/TN and COD/TP in the PDWW increased with an increasing sieve size, verifying the abundance of macromolecules with nitrogen or phosphorous in the small particulate fractions; i.e., higher contents of proteins and lipids were found in the smaller particles. In addition, certain amounts of nutrient elements have to be provided to satisfy the growth requirement of the anaerobic microorganisms. By estimating the net biological growth, the necessitated quantities of the nutrients can be calculated (Rittman and McCarty, 2012). For example, as obtained from stoichiometric equations of a microorganism cell of $C_5H_7O_2NP_{(1/12)}$, N accounts for 12% of the weight of the cell while P accounts for 2%. Here, C indicates biological C, and N should be in the reduced form ($NH_3$-N or organic amino-nitrogen). Hence, concentrations of 5–15 mg N/g COD and 0.8–2.5 mg P/g COD are required in the feed for anaerobic digestion. Because of the effective interception of DMF process, the COD reached 2125.89 ± 273.71 mg/L in the PDWW with $NH_3$-N and TP of 34.58 ± 4.47 mg/L and 11.86 ± 1.02 mg/L, respectively, indicating the presence of a suitable balance among organics and nutrients for anaerobic digestion.

**Fig. 3.**

## *3.3. Comparison of DWW and PDWW*

The size distributions of turbidity, chroma, TSS, VSS, TN, TP, PS, PN, Lip, and COD among the settleable, suspended, super colloidal and colloidal, and dissolved size

fractions of the DWW and PDWW are shown in Fig. 4. The relative abundance of the parameter in each fraction is shown as a percentage (fraction %) of the DWW and PDWW. The differences between the DWW and PDWW are listed follows:

(1) The proportion of settleable matter increased evidently in the PDWW. For the DWW, only 24.3% of the particles existed as settleable matter, and 38.2% of the particles were in suspended form, a similar PSD result was reported in a previous study (van Nieuwenhuijzen et al., 2004). While for PDWW the proportion of settleable matter was 63.4% and the remainder of the content was almost entirely suspended matter with a proportion of 33.8%, and the chroma showed a similar distribution.

(2) The main contributors to TSS in the DWW were suspended and colloidal matters, with proportions of 50.1% and 40.6% respectively. In the PDWW, the settleable matter accounted for 51.5% of the TSS and suspended matter accounted for 38.6%, indicating that large particles were effectively retained in the PDWW.

(3) TN and TP in the DWW were mainly in the dissolved state, in which they had proportions of 79.3% and 73.1%, respectively. However, in the PDWW, these values were only 46.6% and 29.4%, respectively. The percentages of settleable TN and TP increased to 42.6% and 38.0% in the PDWW from 5.7% and 3.4% in the DWW. This illustrates that the DMF process can effectively intercept the scant TN and TP in settleable substances. Furthermore, as mentioned in Section 3.2, because of the interception properties of the DMF process to retain large-size substances, the PDWW had a suitable carbon source and sufficient nutrient quantity for anaerobic digestion (C:

N: P=180: 3: 1).

(4) For COD in the PDWW, the proportions for settleable, suspended, colloidal, and dissolved states were 52.4%, 32.2%, 2.6%, and 12.8%, respectively. The low relative abundance of soluble and colloidal COD can be explained from two aspects: 1) the supporting material with pore size of 25 μm used in DMF process can't retain the solutes and colloids effectively, and they are mostly lost in the filtrate (Xiong et al., 2019); 2) the degradation of soluble and colloidal COD during the DMF preconcentration process.

The results above all indicated effective retention of particles by the DMF process for preconcentration of DWW, especially for the settleable and suspended substances, which are generally removed in the primary settling tank in the traditional CAS process. According to a previous study, approximately 66% of the energy entering the sewage treatment plant is captured in primary sludge (Meerburg et al., 2016); thus, the PDWW realized organic matter recovery to a certain extent. The BMP of substances with large particle size will be discussed in Section 3.5.

**Fig. 4.**

## *3.4. Elements composition in PDWW*

The particles intercepted on the stainless-steel sieves and filter papers for all fractions of the PDWW become progressively more exquisite with decrease of sieve pore size. The SEM images showed that the morphology of particles gradually become more delicate and more even with reduction of sieve pore diameter from 2000 μm to 40 μm.

When the filtering size was reduced from 40 μm to 10 μm, 5 μm, and finally 0.45 μm, some particles looks like crystalline substances appeared, especially in the fractions of 5 μm and 0.45 μm. These may be inorganic salts in the wastewater. The EDX results showed that the main elements detected in the PDWW were C, O, Ca, Na, Mg, Cl, Si, P, S, Fe, and some others, which is similar to the results for DWW in previous studies (Gao et al., 2020; Zhou et al., 2017; Eriksson et al., 2002). Additionally, with decrease of sieve size, the relative abundance of organic matters gradually decreased, whereas the inorganic salt content gradually increased, as shown by the peak intensity, some representative elements of inorganic compounds, such as Na and Cl, increased significantly. The TS of dissolved substances mainly existed as salt crystals. However, because of the EDX analysis only detected TS surface elements, more information about the chemical composition of the TS will be discussed later in the XPS results.

The XPS spectra of PDWW samples of the different fractions was depicted over the energy range of 0–1200 eV. The XPS spectrum is a diagram of the relationship between the number of electrons detected per unit time and the electron binding energy of the elements in the analyzed sample. Each peak corresponds to an electron with the characteristic binding energy of a particular element and the peak intensity is related to the relative abundance of the element (Badireddy et al., 2010). It can be seen that all samples had core-level peaks of C 1s (283.9 eV) and O 1s (531.7 eV). For samples with fractionation size less than 10 μm, 5 μm and 0.45 μm, the signal of Na 1s (1100 eV), along with minor peaks associated with Cl 2p (212 eV), became stronger, which was in

accordance with the EDX results discussed before. The increases of these three elements may be attributed to inorganic salts, such as NaCl in the wastewaters. As the functional groups can determine the position of the associated elemental peak, high-resolution scans of core-level peaks of C 1s and O 1s of raw PDWW were chosen as representatives to investigate and obtain more detailed information on their chemical functionality of the state. The component peaks of C 1s peak can be decomposed into four component peaks (fwhm = 1.23 eV), and the peaks were assigned as follows: (1) a peak at 283.9 eV resulting from C–(C, H), which is mainly from hydrocarbons such as lipids or amino acids side chains (Badireddy et al., 2010); (2) a peak at 285.9 eV due to C–(O, N), which is associated with alcohol, ether, amine, or amide (Badireddy et al., 2008); (3) a peak at 286.9 eV attributable to C=O or O–C–O, as in carboxylate, carbonyl, amide, acetal, or hemiacetal; and (4) a weak peak at 289.0 eV arising from O=C–OH and O=C–OR, which is probably associated with carboxyl or ester groups (Liao et al., 2011).

The O 1s peak was resolved into two peaks (fwhm = 1.83 eV) and different peak areas of each bond indicate their different contents within the TS in the PDWW: (1) a peak at 531.6 eV due mainly to O=C, predominantly from in carboxylate, carbonyl, ester, or amide and (2) a peak at 532.7 eV associated with O–(C, H), including hydroxide, acetal, and hemiacetal.

It has been reported that acetal, hemiacetal, and hydroxide are likely due to carbohydrates, and carboxylate and carboxyl groups indicate the presence of proteins

and acidic carbohydrates (Ma et al., 2013); Amino acids side chains may be the hydrolysates of protein and sugar (Huang et al., 2010); Esters may be derived from DWW containing phthalate plasticizers and food additives containing hydroxybenzoic acid, as well as human excreta, soaps and food oils, and fats (Eriksson et al., 2002). No P 2p peak was observed in all cases, indicating that nucleic acids and phospholipids were below the detection limit of XPS (total P < 0.1%) (Badireddy et al., 2010). All of the analyses above revealed that there is abundant organic matter in the PDWW concentrate, which has the potential to produce methane.

### *3.5. Potential methane production of PDWW*

Fig. 5 shows the results of the accumulative methane production of the raw PDWW and its different fractions. The fitted parameters by the modified Gompertz equation are shown in Table 1. The proportions of methane production of the settleable, suspended, colloidal, and dissolved portions of the PDWW were 58.9%, 27.2%, 8.1%, and 5.8%, respectively, which corresponded perfectly with the COD concentrations of the different fractions ($r_p$ = 0.99). The biomethane production potential ($P_0$) of the raw PDWW was 262.52 ± 11.86 mL $CH_4$/g COD, which was comparable to reported results (Li et al., 2017; Gao et al., 2019) Additionally, the lag time for the different fractions of the PDWW was low, indicating the feasibility of anaerobic digestion of PDWW.

For dissolved matters in the PDWW, the $P_0$ was 131.10 ± 6.19 mL $CH_4$/g COD, showing the lowest methane conversion rate as 37.4%. Though no such study focuses on anaerobic digestion of PDWW based on the size fractionation, similar conclusions

are reached in studies regarding domestic wastewater. The maximum conversion to methane for DWW was 74%, and the maximum conversion of the dissolved fraction was the lowest (62%) (Elmitwalli et al., 2001). Hernández Leal et al. indicated that 70 ± 5% of the COD of the gray water could be biodegraded anaerobically, whereas the biodegradability of SCOD was the lowest (64 ± 12%) (Hernández Leal et al., 2011). The dissolved organic matters can be biodegraded easily will be used by microorganism in pipelines upstream of the WWTP as well as the preconcentration process, and more non-degradable SCOD from the hydrolysis of particles will present in PDWW, hence the biomethane potential will relatively lower compared to the DWW or gray water (Elmitwalli et al., 2001; Ravndal et al., 2018). The $P_0$ of the suspended fraction was the highest with the value of 330.46 ± 2.76 mL $CH_4$/g COD, not only for the abundance of organic substances, such as protein and lipids, in the suspended fraction, but also the ratio of surface area to volume of particles was lower in the suspended fractions, so substrate availability was higher compared to the settable matters. The $P_0$ of settable matters in PDWW was 267.07 ± 16.43 mL $CH_4$/g COD, which can be explained by the limited biodegradability of the larger solid fraction (Dimock and Morgenroth, 2006). The settleable fraction with larger particle size may contain starch, lignin, cellulose, fiber, and so on, which can be from food particles and raw animal fluids from kitchen sinks and soil particles, as well as hair from laundry wastewater. Thus, hydrolysis process will be the limiting step, especially for lignin and cellulose, which can hardly be biodegraded (Xing et al., 2020; Rittman and McCarty, 2012). Hence, the biogas

production potential was relatively lower for the settleable fraction.

**Fig. 5.**

**Table 1**

## *3.6. Implications of resource and energy recovery from PDWW*

Some technical implications of this study from the analysis of the experimental data are listed below:

(1) Compositional analysis performed by combining size fractionation and chemical species analysis is highly recommended during wastewater treatment. Based on compositional analysis with different size fractions, the distribution of macro-pollutants, such as organic matters and nutrients, within different particle size ranges can be clarified. The results obtained can provide a better understanding of the wastewater quality, which is conducive to the design and optimization of the wastewater treatment process and also to the recovery of additional resources. For instance, when preconcentrating organic substances in DWW, as done in this work, the quality and properties of the PDWW can be easily predicted and verified based on the preconcentration process adopted and the compositional analysis. In addition, novel findings pertaining to unconventional resource recovery can be achieved. It has been proven that the inert matter cellulose in DWW exists mainly in the fraction with size larger than 350 μm. After sieving with fine-mesh sieves (< 350 μm), the cellulose fiber mainly from toilet paper can be effectively removed with high recovery and purity (Ruiken et al., 2013). Another study showed that particulate size fractions between 0.65

*and 100 μm contain highly abundant lipids, which can be a good source for oil extraction for biodiesel production (Ravndal et al., 2018). Therefore, compositional analysis based on size fractionation can be a powerful tool for wastewater treatment application.*

*(2) In this work, the characterization of the PDWW indicated that it had larger proportions of settleable (63%) and suspended (34%) fractions in the particle size distribution than the DWW. Although an acceptable average BMP of 262.52 mL $CH_4$/g COD was noted for the PDWW under well-controlled BMP tests, the slow hydrolysis rate of the large particles requires additional attention for practical application of anaerobic digestion of the PDWW, which may be the limiting step in anaerobic digestion. Additionally, the effect will be even worse under lower water temperatures, especially in the case of lignin and cellulose containing substances, which can hardly be biodegraded (Rittman and McCarty, 2012). Therefore, taking appropriate measures such as increasing the anaerobic fermentation temperature, prolonging the hydraulic retention time, exploring the most suitable anaerobic fermentation reactor model, etc., can be alternatives for strengthening the methane production.*

*(3) The organics and nutrients that cannot be concentrated in the permeate of the DMF process require additional concerns. Our previous study assessed the organic matter interception characteristics and COD mass balance of the DWW preconcentration by DMF process (Xiong et al., 2019). Although 12% of the influent COD was lost possibly due to biodegradation and mineralization of organic matter by*

microbes, the DMF process still recovered almost 51% of the organic matter in the DWW. Because of the less effective interception of soluble substances by the DM layer, about 37% of the total COD flowed out with the permeate, which was higher than the values (27% and 19%) in combined coagulation microfiltration systems (Jin et al., 2015; Jin et al., 2016). Soluble organics capture can be enhanced by optimizing preconcentration methods, such as the combined coagulation–microfiltration process. However, in the present study, a lower average BMP of 131.10 mL $CH_4$/g COD for the soluble fraction of the PDWW was observed. Therefore, it is suggested that soluble organics recovery from DWW should be assessed further based on the tradeoff between chemicals (such as coagulants) consumption and residual production and enhancement of bioenergy recovery. On the other hand, because of the low-strength organics and abundant $NH_3$-N and $PO_4^{3-}$-P in the permeate of the DMF process, the permeate can be used for agriculture or landscape irrigation, where energy requirements are significantly lower than for further treatment. Therefore, permeate reuse for irrigation is a likely alternative for capturing the full resource potential of wastewaters, and this alternative should be investigated further.

(4) Wastewater preconcentration integrated with the AD process should be considered carefully as a holistic strategy for large-scale wastewater treatment and resource recovery. To this end, a variety of macro-contaminates (e.g., ammonia and sulfate) and micropollutants, such as endocrine disruptors, pharmaceutical and personal care products, and microplastics, require more scientific attentions during wastewater

treatment. As noted, during sewage preconcentration, the accumulation of high $NH_3$-N in the concentrate may have a negative influence on AD process (Gao et al., 2019; Poirier et al., 2016). Hence the AD performance needs to be enhanced when potential AD inhibitors are enriched. In addition, after wastewater preconcentration, the large amount of filtrate should be reused or post-treated; thus, special concerns should be given to the aforementioned emerging pollutants due to their potential environmental risks.

## 4. Conclusions

Characterization of DWW based on size fractionation is recommended for choosing appropriate wastewater preconcentration methods. The DMF process could effectively retain organic matters in DWW, producing a PDWW with a high COD of 2125.89 ± 273.71 mg/L. The suspended and settleable fractions dominated the particle size and COD distributions, and showed satisfactory BMP values, indicating that it is feasible to use particulate organics captured in PDWW for efficient bioenergy recovery. However, the effective ways to enhance dissolved organics recovery and to realize maximum bioenergy recovery deserve more efforts by taking particulate organics hydrolysis, nutrients balance, and potential inhibitors into considerations.

**Appendix A. Supplementary data**

## Acknowledgements

This study was supported by the Natural Science Foundation of Shaanxi Province (grant no. 2018JQ5054), the Japan Society for the Promotion of Science (JSPS) support

for JSPS Fellows (no. 19F19745), the Shaanxi Provincial Program for Innovative Research Team (grant no. 2019TD-025), and the Sichuan Science and Technology Program (2020YJ0196).

## Reference

[1] Badireddy, A.R., Chellam, S., Gassman, P.L., Engelhard, M.H., Lea, A.S., Rosso, K.M., 2010. Role of extracellular polymeric substances in bioflocculation of activated sludge microorganisms under glucose-controlled conditions. Water Res. 44, 4505–4516. https://doi.org/10.1016/j.watres.2010.06.024

[2] Badireddy, A.R., Korpol, B.R., Chellam, S., Gassman, P.L., Engelhard, M.H., Lea, A.S., Rosso, K.M., 2008. Spectroscopic characterization of extracellular polymeric substances from Escherichia coli and Serratia marcescens: Suppression using sub-inhibitory concentrations of bismuth thiols. Biomacromolecules 9, 3079–3089. https://doi.org/10.1021/bm800600p

[3] Da Ros, C., Conca, V., Eusebi, A.L., Frison, N., Fatone, F., 2020. Sieving of municipal wastewater and recovery of bio-based volatile fatty acids at pilot scale. Water Res. 174, 115633. https://doi.org/10.1016/j.watres.2020.115633

[4] Dignac, M.F., Ginestet, P., Rybacki, D., Bruchet, A., Urbain, V., Scribe, P., 2000. Fate of wastewater organic pollution during activated sludge treatment: Nature of residual organic matter. Water Res. 34, 4185–4194. https://doi.org/10.1016/S0043-1354(00)00195-0

[5] Dimock, R., Morgenroth, E., 2006. The influence of particle size on microbial hydrolysis of protein particles in activated sludge. Water Res. 40, 2064–2074. https://doi.org/10.1016/j.watres.2006.03.011

[6] Elmitwalli, T.A., Soellner, J., De Keizer, A., Bruning, H., Zeeman, G., Lettinga, G., 2001. Biodegradability and change of physical characteristics of particles during anaerobic digestion of domestic sewage. Water Res. 35, 1311–1317. https://doi.org/10.1016/S0043-1354(00)00377-8

[7] Eriksson, E., Auffarth, K., Henze, M., Ledin, A., 2002. Characteristics of grey wastewater. Urban Water 4, 85–104. https://doi.org/10.1016/S1462-0758(01)00064-4

[8] Faust, L., Temmink, H., Zwijnenburg, A., Kemperman, A.J.B., Rijnaarts, H.H.M., 2014. High loaded MBRs for organic matter recovery fromsewage: Effect of solids retention time on bioflocculation and on the role of extracellular polymers. Water Res. 56, 258–266. https://doi.org/10.1016/j.watres.2014.03.006

[9] Gao, Y., Fang, Z., Chen, C., Zhu, X., Liang, P., Qiu, Y., Zhang, X., 2020. Evaluating the performance of inorganic draw solution concentrations in an anaerobic forward osmosis membrane bioreactor for real municipal sewage treatment. Bioresour. Technol. 307, 123254. https://doi.org/10.1016/j.biortech.2020.123254

[10] Gao, Y., Fang, Z., Liang, P., Huang, X., 2018. Direct concentration of municipal sewage by forward osmosis and membrane fouling behavior. Bioresour. Technol. 247, 730–735. https://doi.org/10.1016/j.biortech.2017.09.145

[11] Gao, Y., Fang, Z., Liang, P., Zhang, X., Qiu, Y., Kimura, K., Huang, X., 2019. Anaerobic digestion performance of concentrated municipal sewage by forward osmosis membrane: Focus on the impact

of salt and ammonia nitrogen. Bioresour. Technol. 276, 204–210. https://doi.org/10.1016/j.biortech.2019.01.016

[12] Gaudy, A.F., 1962. Colorimetric determination of protein and carbohydrate. Ind. Water Wastes 7, 17–22.

[13] Hernández Leal, L., Temmink, H., Zeeman, G., Buisman, C.J.N., 2011. Characterization and anaerobic biodegradability of grey water. Desalination 270, 111–115. https://doi.org/10.1016/j.desal.2010.11.029

[14] Hu, Y., Yang, Y., Yu, S., Wang, X.C., Tang, J., 2018. Psychrophilic anaerobic dynamic membrane bioreactor for domestic wastewater treatment: Effects of organic loading and sludge recycling. Bioresour. Technol. 270, 62–69. https://doi.org/10.1016/j.biortech.2018.08.128

[15] Huang, M.H., Li, Y.M., Gu, G.W., 2010. Chemical composition of organic matters in domestic wastewater. Desalination 262, 36–42. https://doi.org/10.1016/j.desal.2010.05.037

[16] Jimenez, J., Miller, M., Bott, C., Murthy, S., De Clippeleir, H., Wett, B., 2015. High-rate activated sludge system for carbon management - Evaluation of crucial process mechanisms and design parameters. Water Res. 87, 476–482. https://doi.org/10.1016/j.watres.2015.07.032

[17] Jin, Z., Gong, H., Temmink, H., Nie, H., Wu, J., Zuo, J., Wang, K., 2016. Efficient sewage pre-concentration with combined coagulation microfiltration for organic matter recovery. Chem. Eng. J. 292, 130–138. https://doi.org/10.1016/j.cej.2016.02.024

[18] Jin, Z., Gong, H., Wang, K., 2015. Application of hybrid coagulation microfiltration with air backflushing to direct sewage concentration for organic matter recovery. J. Hazard. Mater. 283, 824–831. https://doi.org/10.1016/j.jhazmat.2014.10.038

[19] Joel, N.D., Okabe, S., 2020. Domestic wastewater treatment and energy harvesting by serpentine up-flow MFCs equipped with PVDF-based activated carbon air-cathodes and a low voltage booster. Chem. Eng. J. 380, 122443. https://doi.org/10.1016/j.cej.2019.122443

[20] Lateef, S.K., Soh, B.Z., Kimura, K., 2013. Direct membrane filtration of municipal wastewater with chemically enhanced backwash for recovery of organic matter. Bioresour. Technol. 150, 149–155. https://doi.org/10.1016/j.biortech.2013.09.111

[21] Lei, Z., Yang, S., Li, Y. you, Wen, W., Wang, X.C., Chen, R., 2018. Application of anaerobic membrane bioreactors to municipal wastewater treatment at ambient temperature: A review of achievements, challenges, and perspectives. Bioresour. Technol. 267, 756–768. https://doi.org/10.1016/j.biortech.2018.07.050

[22] Li, S., Yang, Y., Hu, Y., Tang, J., Wang, X.C., 2017. Development of a novel two-stage powdered activated carbon-dynamic membrane filtration ( PAC-DMF ) system for direct physicochemical wastewater treatment. Desalin. Water Treat. 99, 299–308. https://doi.org/10.5004/dwt.2017.21750

[23] Liao, B.Q., Lin, H.J., Langevin, S.P., Gao, W.J., Leppard, G.G., 2011. Effects of temperature and dissolved oxygen on sludge properties and their role in bioflocculation and settling. Water Res. 45, 509–520. https://doi.org/10.1016/j.watres.2010.09.010

[24] Liu, H., Gu, J., Wang, S., Zhang, M., Liu, Y., 2020. Performance, membrane fouling control and cost analysis of an integrated anaerobic fixed-film MBR and reverse osmosis process for municipal wastewater reclamation to NEWater-like product water. J. Memb. Sci. 593, 117442. https://doi.org/10.1016/j.memsci.2019.117442

[25] Lowry, O.H., Rosebrough, N.J., Farr, A.L., Randall, R.J., 1951. Protein measurement with the Folin phenol reagent. J. Biol. Chem. 193, 265–275.

[26] Ma, J., Wang, Z., Xu, Y., Wang, Q., Wu, Z., Grasmick, A., 2013. Organic matter recovery from municipal wastewater by using dynamic membrane separation process. Chem. Eng. J. 219, 190–199. https://doi.org/10.1016/j.cej.2012.12.085

[27] McCarty, P.L., Bae, J., Kim, J., 2011. Domestic wastewater treatment as a net energy producer-can this be achieved? Environ. Sci. Technol. 45, 7100–7106. https://doi.org/10.1021/es2014264

[28] Meerburg, F.A., Boon, N., Van Winckel, T., Pauwels, K.T.G., Vlaeminck, S.E., 2016. Live fast, die young: Optimizing retention times in high-rate contact stabilization for maximal recovery of organics from wastewater. Environ. Sci. Technol. 50, 9781–9790. https://doi.org/10.1021/acs.est.6b01888

[29] N.E.P.A. Chinese, 2002. Water and Wastewater Monitoring Methods, 4th ed. Chinese Environmental Science Publishing House, Beijing, China.

[30] Ortega-Bravo, J.C., Ruiz-Filippi, G., Donoso-Bravo, A., Reyes-Caniupán, I.E., Jeison, D., 2016. Forward osmosis: Evaluation thin-film-composite membrane for municipal sewage concentration. Chem. Eng. J. 306, 531–537. https://doi.org/10.1016/j.cej.2016.07.085

[31] Poirier, S., Desmond-Le Quéméner, E., Madigou, C., Bouchez, T., Chapleur, O., 2016. Anaerobic digestion of biowaste under extreme ammonia concentration: Identification of key microbial phylotypes. Bioresour. Technol. 207, 92–101. https://doi.org/10.1016/j.biortech.2016.01.124

[32] Ravndal, K.T., Opsahl, E., Bagi, A., Kommedal, R., 2018. Wastewater characterisation by combining size fractionation, chemical composition and biodegradability. Water Res. 131, 151–160. https://doi.org/10.1016/j.watres.2017.12.034

[33] Rittman, B.E., McCarty, P.L., 2012. Environmental Biotechnology: Principals and Applications (Photocopy). Tsinghua University Press, Beijing, China.

[34] Ruiken, C.J., Breuer, G., Klaversma, E., Santiago, T., van Loosdrecht, M.C.M., 2013. Sieving wastewater - Cellulose recovery, economic and energy evaluation. Water Res. 47, 43–48. https://doi.org/10.1016/j.watres.2012.08.023

[35] Sarpong, G., Gude, V.G., Magbanua, B.S., 2019. Energy autarky of small scale wastewater treatment plants by enhanced carbon capture and codigestion – A quantitative analysis. Energy Convers. Manag. 199, 111999. https://doi.org/10.1016/j.enconman.2019.111999

[36] Sophonsiri, C., Morgenroth, E., 2004. Chemical composition associated with different particle size fractions in municipal, industrial, and agricultural wastewaters. Chemosphere 55, 691–703. https://doi.org/10.1016/j.chemosphere.2003.11.032

[37] Sun, Y., Chen, Z., Wu, G., Wu, Q., Zhang, F., Niu, Z., Hu, H.Y., 2016. Characteristics of water quality of municipal wastewater treatment plants in China: Implications for resources utilization and management. J. Clean. Prod. 131, 1–9. https://doi.org/10.1016/j.jclepro.2016.05.068

[38] van Nieuwenhuijzen, A.F., van der Graaf, J.H.J.M., Kampschreur, M.J., Mels, A.R., 2004. Particle related fractionation and characterisation of municipal wastewater. Water Sci. Technol. 50, 125–132. https://doi.org/10.2166/wst.2004.0704

[39] Wang, G., Li, Q., Gao, X., Wang, X.C., 2018. Synergetic promotion of syntrophic methane production from anaerobic digestion of complex organic wastes by biochar: Performance and

associated mechanisms. Bioresour. Technol. 250, 812–820. https://doi.org/10.1016/j.biortech.2017.12.004

[40] Xing, B.S., Han, Y., Cao, S., Wen, J., Zhang, K., Yuan, H., Wang, X.C., 2020. Cosubstrate strategy for enhancing lignocellulose degradation during rumen fermentation in vitro: Characteristics and microorganism composition. Chemosphere 250, 126104. https://doi.org/10.1016/j.chemosphere.2020.126104

[41] Xiong, J., Yu, S., Hu, Y., Yang, Y., Wang, X.C., 2019. Applying a dynamic membrane filtration (DMF)process for domestic wastewater preconcentration: Organics recovery and bioenergy production potential analysis. Sci. Total Environ. 680, 35–43. https://doi.org/10.1016/j.scitotenv.2019.05.080

[42] Yang, X., Wei, J., Ye, G., Zhao, Y., Li, Z., Qiu, G., Li, F., Wei, C., 2020. The correlations among wastewater internal energy, energy consumption and energy recovery/production potentials in wastewater treatment plant: An assessment of the energy balance. Sci. Total Environ. 714, 136655. https://doi.org/10.1016/j.scitotenv.2020.136655

[43] Yang, Y., Zang, Y., Hu, Y., Wang, X.C., Ngo, H.H., 2020. Upflow anaerobic dynamic membrane bioreactor (AnDMBR) for wastewater treatment at room temperature and short HRTs: Process characteristics and practical applicability. Chem. Eng. J. 383, 123186. https://doi.org/10.1016/j.cej.2019.123186

[44] Zhou, L., Zhuang, W.-Q., Wang, X., Yu, K., Yang, S., Xia, S., 2017. New insights into comparison between synthetic and practical municipal. Bioresour. Technol. 244, 934–940. https://doi.org/http://dx.doi.org/10.1016/j.biortech.2017.08.069

## Figure captions and tables

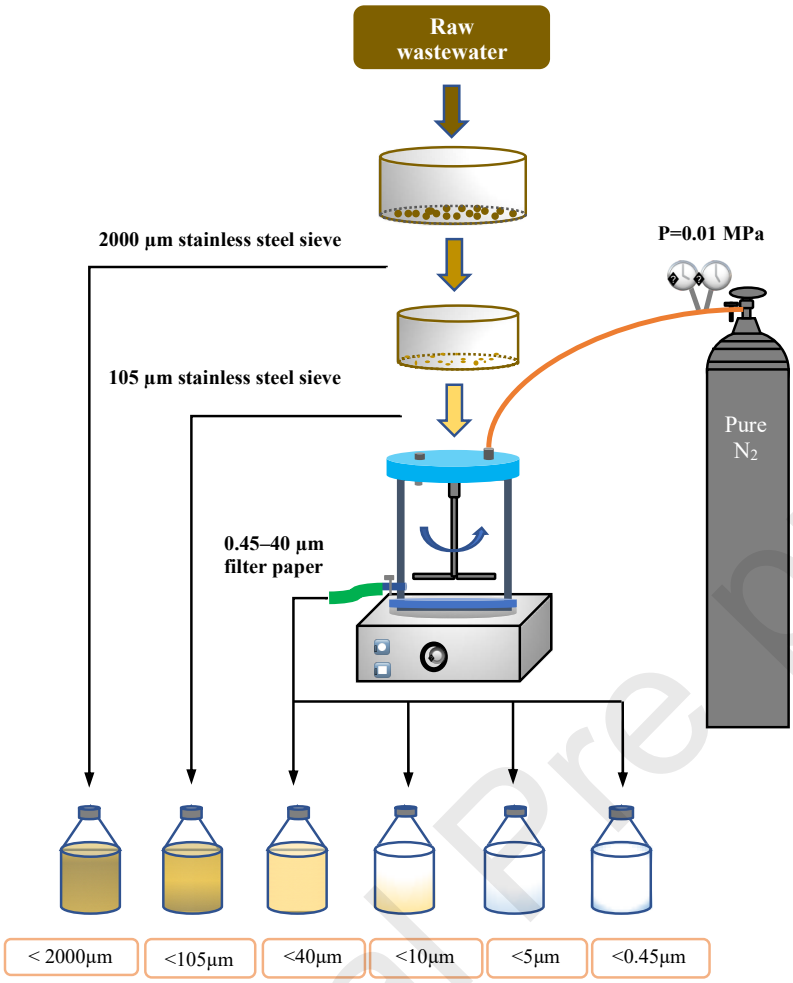


**Fig. 1.** Schematic representation of the wastewater fractionation procedures

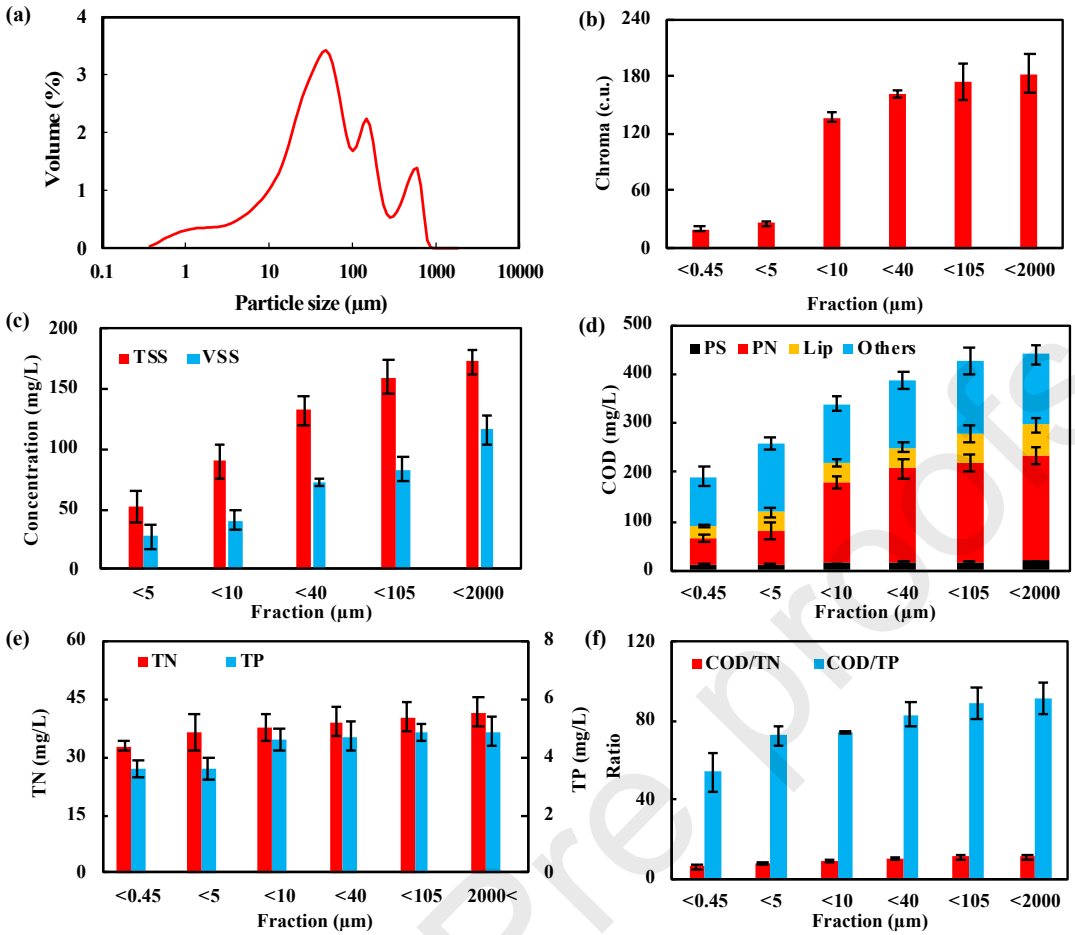


**Fig. 2.** Basic parameters of PSD (a), chroma (b), concentration of TSS and VSS (c), COD compositions (d), concentration of TN and TP (e), and ratios of COD/TN and COD/TP (f) of raw DWW of all fractions. Data are expressed as mean ± standard deviation (n = 4).

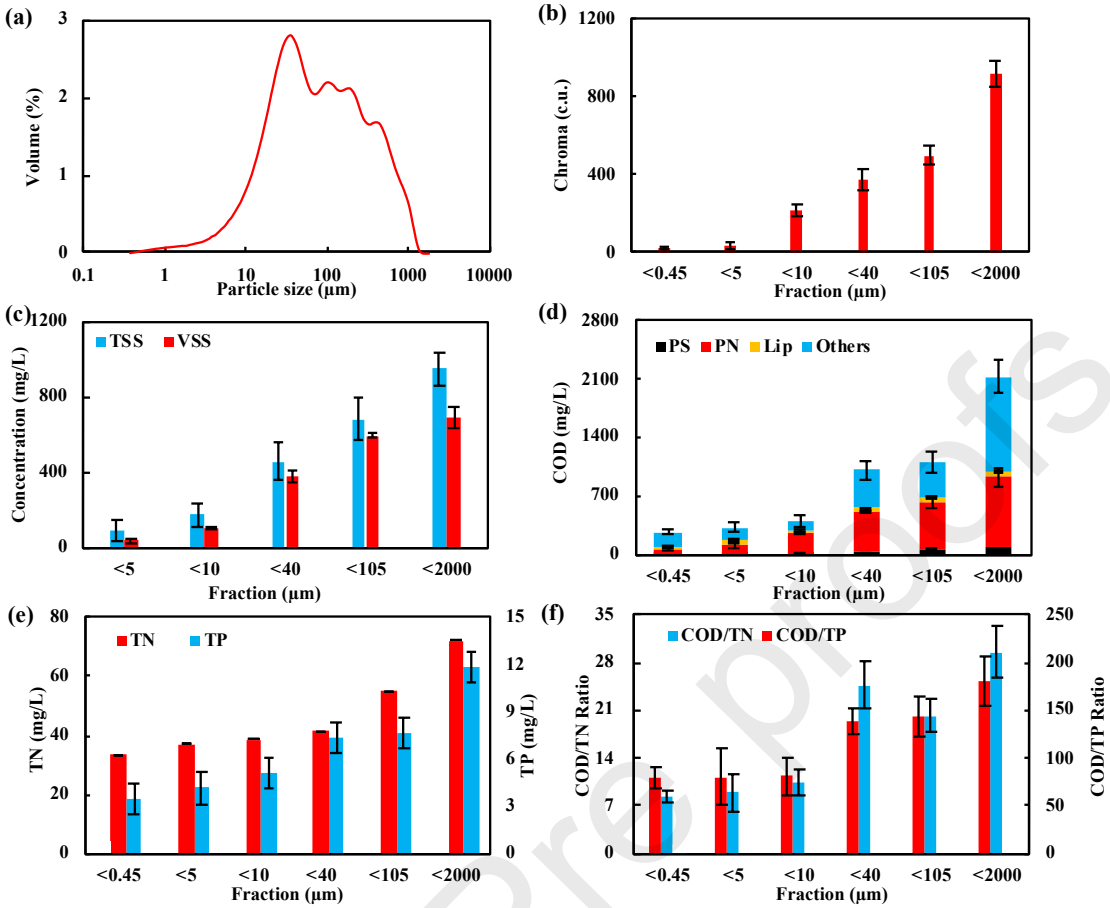


**Fig. 3.** Basic parameters of PSD (a), chroma (b), concentrations of TSS and VSS (c), COD compositions (d), concentrations of TN and TP (e), and ratios of COD/TN and COD/TP (f) for all fractions of the PDWW. Data are expressed as mean ± standard deviation (n = 4).

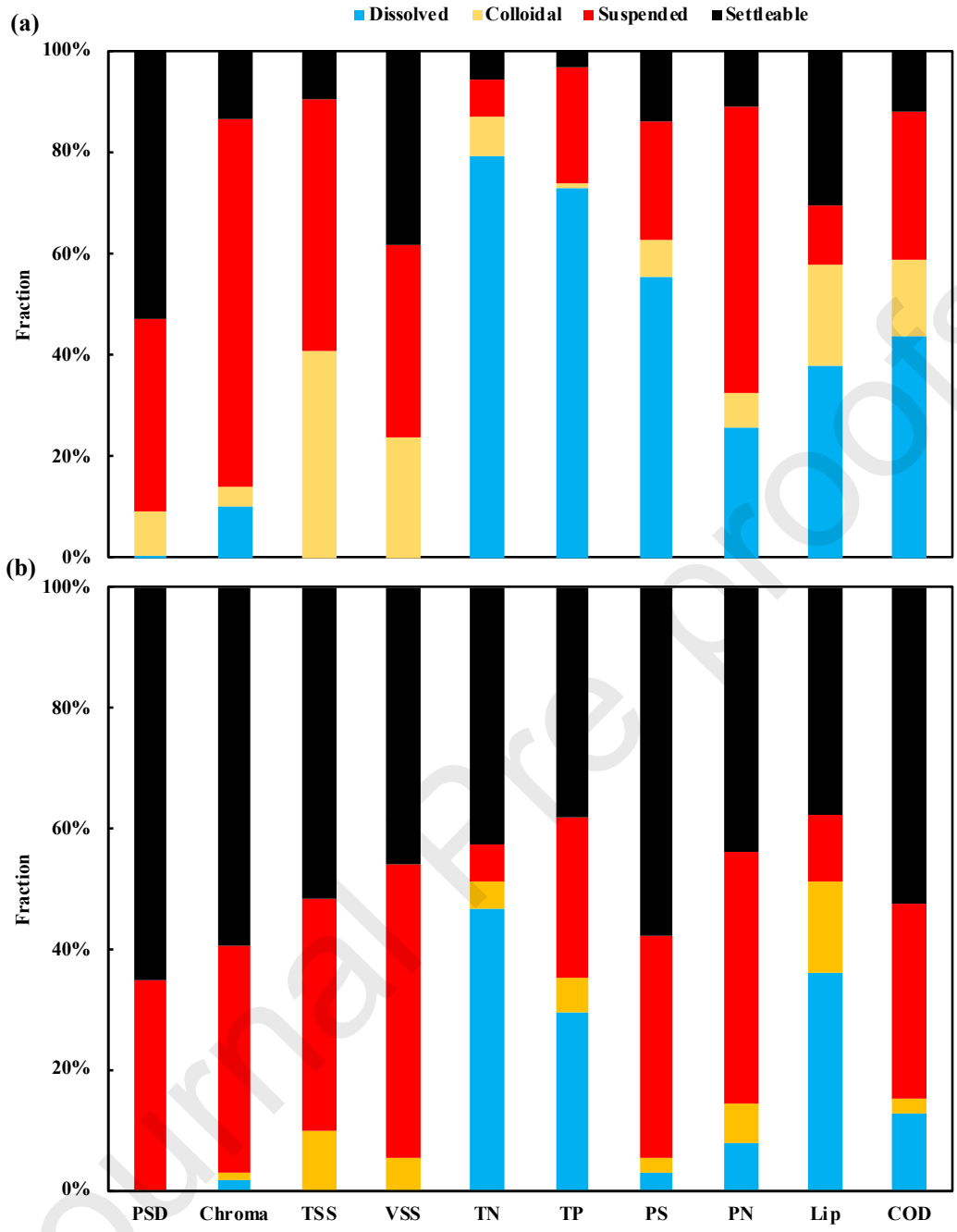


**Fig. 4.** Size distribution of different parameters in settleable (> 40 μm), suspended (5–40μm), super colloidal and colloidal (0.45–5 μm), and dissolved (< 0.45 μm) size ranges in DWW (a) and PDWW (b).

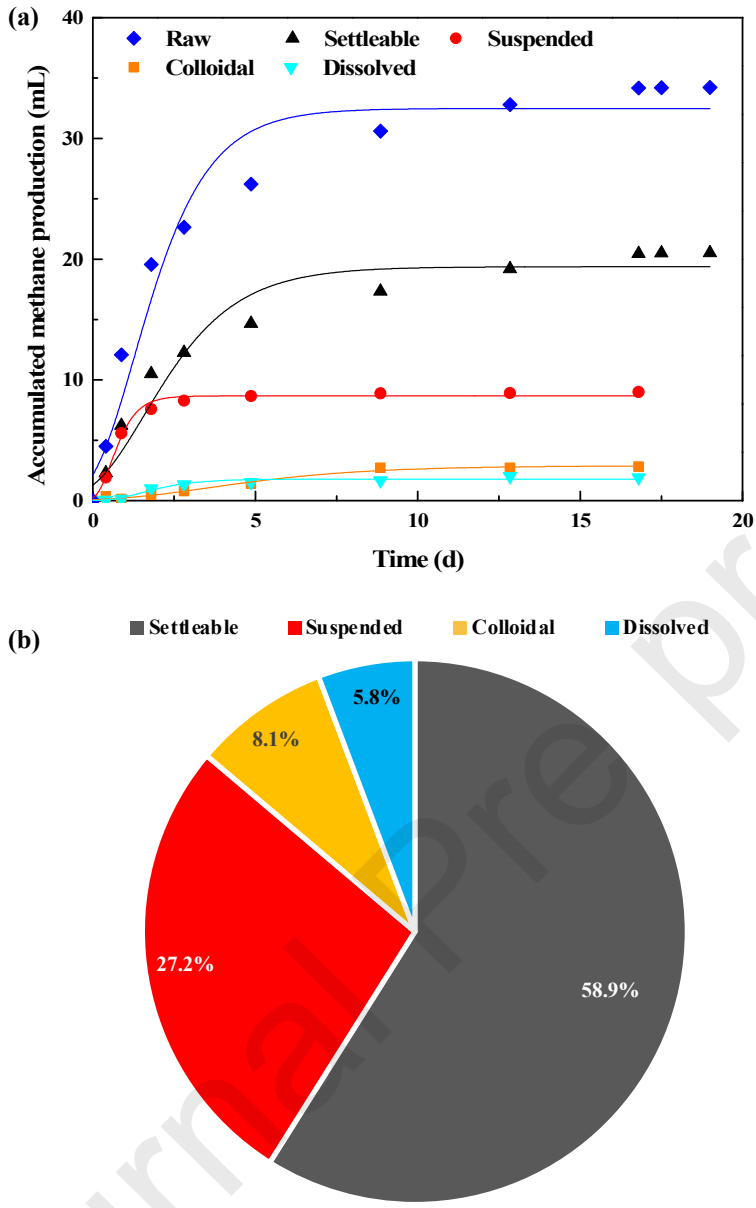


**Fig. 5.** Accumulated methane production (a) and proportion (b) of PDWW in all fractions (expressed as the average value, n = 3).

**Table 1** Fitting results of methane production of PDWW by the modified Gompertz equation.

| Group | $P_0$ (mL $CH_4$/gCOD) | $R_{max}$ (mL $CH_4$/gCOD/d) | $t_0$ (d) | $R^2$ |
|---|---|---|---|---|
| PDWW | 262.52 ± 11.86 | 70.06 ± 20.96 | 0.35 ± 0.45 | 0.942 |
| Settleable | 267.07 ± 16.43 | 68.33 ± 4.85 | 0.52 ± 0.09 | 0.916 |
| Suspended | 330.46 ± 2.76 | 239.80 ± 27.63 | 0.14 ± 0.08 | 0.995 |
| Colloidal | 277.92 ± 5.91 | 95.11 ± 50.92 | 0.76 ± 0.82 | 0.996 |
| Dissolved | 131.10 ± 6.19 | 27.34 ± 5.88 | 0.27 ± 0.39 | 0.998 |



# Highlights

- Characterization of wastewater by fractionation, chemical, degradability analysis
- Proteins, polysaccharides and lipids are major organic components in DWW
- Suspended and settleable solids in PDWW are 33.8% and 63.4% in PSD
- PDWW shows a biomethane production potential of 262.52 ± 11.86 mL $CH_4$/g COD